Use of circular cylinders as surrogates for hexagonal pristine ice crystals in scattering calculations at infrared wavelengths

Yong-Keun Lee, Ping Yang, Michael I. Mishchenko, Bryan A. Baum, Yong X. Hu, Hung-Lung Huang, Warren J. Wiscombe, and Anthony J. Baran

We investigate the errors associated with the use of circular cylinders as surrogates for hexagonal columns in computing the optical properties of pristine ice crystals at infrared (8–12-μm) wavelengths. The equivalent circular cylinders are specified in terms of volume (V), projected area (A), and volume-to-area ratio that are equal to those of the hexagonal columns. We use the T-matrix method to compute the optical properties of the equivalent circular cylinders. We apply the finite-difference time-domain method to compute the optical properties of hexagonal ice columns smaller than 40 μm. For hexagonal columns larger than 40 μm we employ an improved geometric optics method and a stretched scattering potential technique developed in previous studies to calculate the phase function and the extinction (or absorption) efficiency, respectively. The differences between the results for circular cylinders and hexagonal columns are of the order of a few percent. Thus it is quite reasonable to use a circular cylinder geometry as a surrogate for pristine hexagonal ice columns for scattering calculations at infrared (8–12-μm) wavelengths. Although the pristine ice crystals can be approximated as circular cylinders in scattering calculations at infrared wavelengths, it is shown that optical properties of individual aggregates cannot be well approximated by those of individual finite columns or cylinders. © 2003 Optical Society of America

OCIS codes: 010.1290, 010.1310, 010.3920, 290.5850, 290.1090, 280.1310.

1. Introduction

It is quite challenging to assess quantitatively the radiative effect of cirrus clouds in the atmosphere.[1–3] One of the major difficulties encountered in modeling the radiative properties of cirrus clouds is that these clouds are composed almost exclusively of nonspherical ice crystals. Although various ice crystal configurations, including hexagonal columns, plates, hollow columns, bullet rosettes, and aggregates, have been observed,[4–7] it is a common practice to assume that the geometry of ice crystals is that of hexagonal columns in climate and remote-sensing applications.[8–11] This simplification is based mainly on two facts: First, the halos observed at visible wavelengths are scattering characteristics that are typical of a hexagonal crystal geometry, although it has been argued that halos are not often observed in the atmosphere (see, e.g., Foot[12]). Second, pristine ice crystals that form at extremely cold temperatures, such as in cirrus clouds and polar stratospheric clouds, tend to have basic hexagonal structures. Various parameterization efforts and radiative sensitivity studies assume a hexagonal geometry for ice crystals in cirrus clouds. However, in a few recent studies a mixture of various ice crystal configurations was assumed,[13–18] but those studies were essentially limited to the solar spectrum.

At solar wavelengths, particularly at visible wavelengths, the scattering properties of hexagonal ice crystals can be approximated by use of the geometric optics ray-tracing method. At infrared wave-

Y.-K. Lee and P. Yang (pyang@ariel.met.tamu.edu) are with the Department of Atmospheric Sciences, Texas A&M University, College Station, Texas 77843. M. I. Mishchenko is with the NASA Goddard Institute for Space Studies, 2880 Broadway, New York, New York 10025. B. A. Baum and Y. X. Hu are with the NASA Langley Research Center, MS 420, Hampton, Virginia 23681. H.-L. Huang is with the Cooperative Institute for Meteorological Satellite Studies, University of Wisconsin—Madison, 1225 West Dayton Street, Madison, Wisconsin 53706. W. J. Wiscombe is with NASA Goddard Space Flight Center, Code 913, Greenbelt, Maryland 2077. A. J. Baran is with the Met Office, Bracknell, Berkshire, RG12 2 SZ, UK.

Received 24 September 2002; revised manuscript received 6 January 2003.

0003-6935/03/152653-12$15.00/0

© 2003 Optical Society of America

lengths, for which the sizes of ice crystals are not substantially larger than the incident wavelength, the geometric optics method breaks down. In addition, ice crystals have strong absorption at infrared wavelengths. Because of the substantial absorption within ice crystals at infrared wavelengths, the electromagnetic wavelengths refracted into ice crystals are inhomogeneous waves.[19,20] The inhomogeneity of the refracted electromagnetic wave can significantly complicate the ray-tracing computation and degrade the accuracy of the conventional ray-tracing technique.[21] Therefore, accurate scattering computational methods must be used in calculating the scattering properties of ice crystals at infrared wavelengths. The finite-difference time-domain (FDTD) method[22–25] and the discrete dipole approximation[26–28] (DDA) are accurate numerical methods that can be applied to an arbitrarily shaped particle, assuming that a sufficiently fine resolution is used for the grid meshes (FDTD) or the sizes of the dipole elements (DDA). However, these two methods require extremely large computational resources in terms of computer CPU time and memory. The applicability of the FDTD and the DDA is quite limited in practice, particularly when scattering calculations are required for various size parameters and multiple wavelengths. The T-matrix method, if it is implemented for axisymmetric particles, is the most computationally efficient method available now for accurately computing the single-scattering properties of nonspherical particles.[29]

In the present study we ascertain the accuracy of using circular cylinders as surrogates for computation of the scattering properties of hexagonal ice crystals at infrared wavelengths. The hexagonal geometry is regarded as more complex than the circular cylinder geometry, as the former has a lower degree of symmetry. The accuracy of using a simpler geometry as a surrogate for a more-complex geometry in light-scattering computations was investigated in several previous studies. Liou and Takano[30] showed that an equivalent sphere with the same surface area or the same volume does not reproduce the proper single-scattering properties of hexagonal ice crystals at infrared wavelengths. Chylek and Videen[31] also showed that the equivalent spheres of equal volume or equal surface area are not suitable for approximating hexagonal columns or plates. Macke and Mishchenko[32] investigated the accuracy of approximating a hexagonal geometry by using ellipsoidal and circular cylinders in light-scattering calculations at visible and near-infrared wavelengths. Those authors found substantial differences in light-scattering calculations for three geometries (hexagonal, ellipsoidal, and circular cylinder particles) at a nonabsorbing wavelength (e.g., 0.55 μm) and recommended against the substitution of ellipsoidal and circular cylinder geometries for the hexagonal structure. However, for the integrated scattering properties such as the asymmetry factor at absorbing wavelengths (e.g., 1.6 and 3.7 μm), the overall differences among the three geometries are much smaller in magnitude. Kahnert *et al.*[33] investigated the accuracy of approximating an ensemble of wavelength-sized prisms by spheroids and cylinders in light-scattering calculations based on the extended boundary condition method. Their results show that the optical properties of cylinders are closer to those of prisms than of spheroids. Baran *et al.*[34] investigated the accuracy of using a size–shape distribution of randomly oriented circular ice cylinders to simulate scattering from a distribution of randomly oriented ice aggregates. Grenfell and Warren[35] suggested that a nonspherical particle can be approximated by a collection of monodisperse spheres that have the same volume-to-surface (V/A) ratio. Those authors also carried out intensive validation studies of the accuracy of their method for calculating the bulk optical properties of ice crystals and modeling radiative transfer processes that involve ice clouds. The present study is an extension of that of Grenfell and Warren[35] in the sense that a simpler geometry is used to approximate a more-complex geometry for scattering and absorption computations.

Motivated by the computational efficiency of the T-matrix method when it is applied to a circular cylinder geometry with small and moderate size parameters, one may inquire whether a hexagonal geometry can be approximated by a circular cylinder at infrared wavelengths with acceptable errors in the scattering properties. From physical intuition, one may expect that the detailed sharp edges of side faces of a hexagon may not be so important in light-scattering calculations in the infrared region because of strong absorption within the particle and because the wavelength is of the same order as the particle size. In addition, in the atmosphere the surface edges of pristine ice crystals may be rounded owing to sublimation or riming.[32] Thus an investigation of the scattering properties of circular cylinders may be interesting in its own right. The efficient computation of single-scattering properties for circular cylinders by the T-matrix method may provide the optical properties of small ice crystals and also provide a data set for constructing the approximate optical properties of large particles based on the composite method developed by Fu *et al.*,[36,37] which is one of the most practical approaches available for covering a wide range of size parameters.

This paper is organized as follows. In Section 2 we present the approach used for light-scattering calculations. Seven ways to approximate a hexagonal geometry by a circular cylinder are presented. Numerical computations and an associated discussion are provided in Section 3. Finally, conclusions are given in Section 4.

2. Approach

In the present study we use the T-matrix computation program developed by Mishchenko[38] to calculate the single-scattering properties of randomly oriented circular cylinders. A detailed description of the T-matrix method and documentation of the compu-

tational program have been provided by Mishchenko and Travis[39] and will not be reiterated here. The T-matrix method pioneered by Waterman[40] can be applied in principle to any arbitrary geometry. The application of the T-matrix method based on the extended boundary condition method for rotationally symmetric shapes can be traced back to the studies of Wiscombe and Mugnai,[41] Barber and Hill,[42] and Mishchenko and Travis.[39] Recently the numerical implementation of this method was extended to geometries other than axisymmetric particles.[43–45] Havemann and Baran[46] employed the T-matrix method to compute the single-scattering properties of hexagonal ice crystals with size parameters up to 40. In the numerical computation, the applicable size parameter region of the T-matrix, if it is implemented as a nonaxisymmetric geometry, is usually narrower than for axisymmetric particles. A combination of the T-matrix method and other numerical light-scattering computational methods, such as the DDA and the FDTD, may shed new light on efficient computation of the optical properties of nonspherical particles.[47,48] In practice, the analytical approach of averaging the effect of particle orientations in the T-matrix method[49] can substantially speed up numerical computations.

To ascertain the difference in the optical properties of hexagonal and circular cylindrical ice crystals we take the extinction efficiency, the single-scattering albedo, the phase function, and the asymmetry factor calculated by Yang *et al.*[50] as the reference data set. In that study the FDTD method was applied to small hexagonal ice crystals with maximum dimensions smaller than 40 μm. For the computation of the asymmetry factor, Yang *et al.*[50] used a combination of the FDTD method and an improved geometric optics method (for particle sizes larger than 40 μm) to compute the phase function. In the computation of extinction and absorption efficiencies, the stretched scattering potential method (SSPM) is applied to ice crystals with maximum dimensions larger than 40 μm. The SSPM results are refined by the weighted summation of the SSPM, the Lorenz–Mie solution for equivalent spheres, and the geometric optics solution in a manner similar to the composite approach developed by Fu *et al.*[36] When the FDTD and the refined SSPM solutions are combined, the results computed by Yang *et al.*[50] encompass ice crystal sizes specified in terms of their maximum dimensions from 1 to 10000 μm.

In the present study we consider particle sizes that range from 1 to 180 μm. Over this size range, the T-matrix method gives convergent solutions in the 8–12-μm spectral region. For a given maximum dimension, the aspect ratio given by Yang *et al.*[50] is followed, which is

$$2a/L = \begin{cases} 1 & L \le 40\ \mu\text{m} \\ \exp[-0.017835(L-40)] & 40\ \mu\text{m} < L \le 50\ \mu\text{m} \\ 5.916/L^{1/2} & L > 50\ \mu\text{m} \end{cases}, \tag{1}$$

where a is the semiwidth of the cross section and L is the length of a hexagonal column. Ice crystals defined by Eq. (1) are compact hexagons with aspect ratios of unity if their maximum dimensions are smaller than 40 μm, whereas crystals larger than 40 μm are essentially hexagonal columns.

The radius of the cross section and the length of a circular cylinder are denoted R and H, respectively. To define an equivalent circular cylinder for a hexagonal particle, one can assume that the two particles have the same projected area, volume, or ratio of volume to projected area under the condition that the two particles have the same length or aspect ratio. If circular and hexagonal cylinders have the same length (i.e., $H = L$), the radius of the circular cylinder with the same volume is given by

$$R_v = \sqrt{\frac{3\sqrt{3}}{2\pi}}\, a, \tag{2}$$

where the subscript v indicates that the circular cylinder has the same volume as the hexagon. The cross-sectional radius of a circular cylinder with the same projected area as the hexagon is given by

$$R_a = \frac{[L^2 + (6\sqrt{3}a^2 + 12aL)/\pi]^{1/2} - L}{2}. \tag{3}$$

Similarly, the cross-sectional radius of the circular cylinder that has the same ratio of volume to projected area as a hexagon is given by

$$R_{v/a} = \frac{\sqrt{3}}{2}\, a. \tag{4}$$

To define the equivalence of a circular cylinder and a hexagonal column in scattering calculations, one can also let the two particles have the same aspect ratio, that is, $a/L = R/H$. For this condition the cross-sectional radius of a circular cylinder with an equivalent volume, an equivalent projected area, or an equivalent ratio of volume to projected area is given by

$$R_v^* = \left(\frac{3\sqrt{3}}{2\pi}\right)^{1/3} a, \tag{5}$$

$$R_a^* = \left[\frac{3\sqrt{3}a + 6L}{2\pi(a+L)}\right]^{1/2} a, \tag{6}$$

$$R_{v/a}^* = \frac{\sqrt{3}(a+L)}{\sqrt{3}a + 2L}\, a. \tag{7}$$

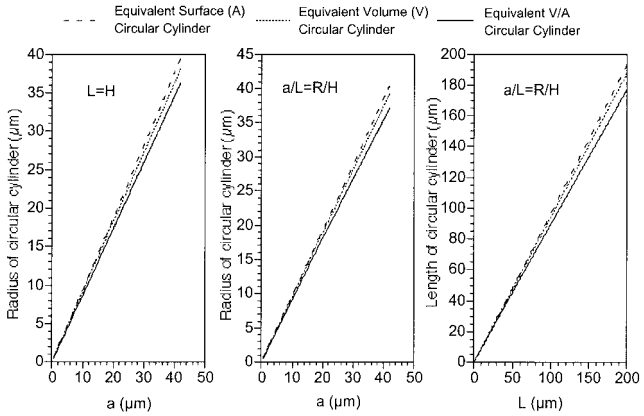

Fig. 1. Radii and lengths of circular cylinders defined as having the same volume, surface area, or ratio of volume to surface area as hexagonal columns when the same length or aspect ratio is applied to the two geometries. Left, same lengths of circular cylinders and hexagonal columns; Middle and right, aspect ratio kept constant in defining the equivalence.

The lengths associated with the radii in Eqs. (5)–(7) are given by

$$H_v^* = \left(\frac{3\sqrt{3}}{2\pi}\right)^{1/3} L, \tag{8}$$

$$H_a^* = \left[\frac{3\sqrt{3}a + 6L}{2\pi(a + L)}\right]^{1/2} L, \tag{9}$$

$$H_{v/a}^* = \frac{\sqrt{3}(a + L)}{\sqrt{3}a + 2L} L. \tag{10}$$

Figure 1 shows the radii and lengths defined in Eqs. (3)–(7) versus semiwidth (a) and length (L) of a hexagonal column. The aspect ratio defined in Eq. (1) is used for defining the semiwidth of the cross section of a hexagonal column of a given length. At the left in Fig. 1 the radius of a circular cylinder with the same surface (A), volume (V), or ratio of volume to surface area (V/A) as a hexagonal column when the lengths of the two geometries are the same is shown. Evidently, the circular cylinder specified on the basis of surface-area equivalence is largest, whereas that based on V/A equivalence is smallest in terms of the radius of cross section. In the middle and at the right in Fig. 1 are the radii and lengths of cylinders with aspect ratios that are the same as for the hexagonal crystals.

3. Numerical Results and Discussion

The results presented here focus on the scalar optical properties of scattering particles, including extinction efficiency, absorption efficiency, phase function, and asymmetry factor. Similarly to Yang *et al.*,[50] we use the refractive index compiled by Warren[51] in our numerical computations. The T-matrix computational code is implemented with the extended double precision algorithm.[52]

Figure 2 shows a comparison of the phase functions

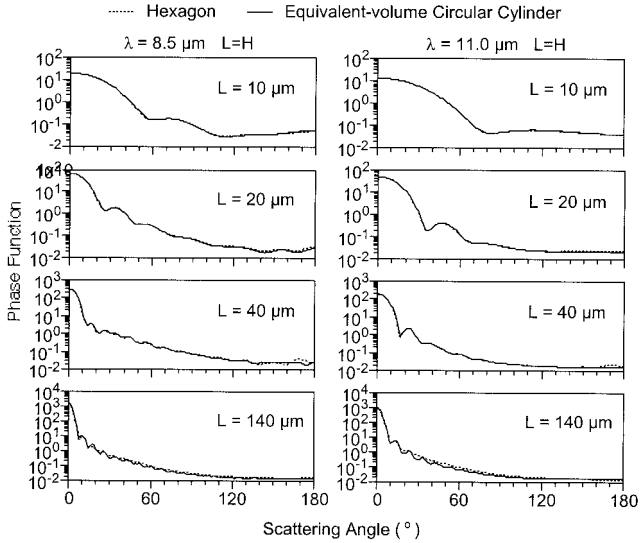

Fig. 2. Comparison of phase functions of circular cylinders and hexagonal columns. The circular cylinders are defined to have the same volume and length as the hexagonal columns. The results for circular cylinders are computed by Mishchenko's T-matrix code.[38] For hexagonal columns the FDTD method is used for small particles (L = 10, 20, 40 μm), whereas an improved geometric optics method is used for L = 140 μm.

of hexagonal ice columns and circular ice cylinders. The circular cylinders are defined to have the same length and volume as the hexagonal columns. For sizes L = 10, 20, 40 μm, the phase functions of the hexagonal columns are computed by the FDTD method, whereas the results for L = 140 μm are computed with an improved geometric optics method. For small sizes, the phase functions of circular cylinders are essentially the same as those of hexagonal columns. The slight differences between the two results near backscattering angles for L = 40 μm might be caused by the inaccuracy of the FDTD method because of insufficient resolution for the grid mesh. The performance of the FDTD method for hexagonal ice crystals was recently assessed by Baran *et al.*[53] in comparison with the implementation of the T-matrix method in a hexagonal geometry. From Fig. 2 excellent agreement between the results at L = 140 μm can be noted. Evidently, the sharp edges of side faces of hexagonal geometry are not important in specifying the optical properties of the particles. Instead, the overall morphology of the particle as a cylinder or a column is the major factor that affects the particle's optical properties.

For infrared radiative transfer simulations, the phase function of cirrus particles can be approximated by the Henyey–Greenstein (H-G) function, given by

$$P_{\text{H-G}}(\theta) = \frac{1 - g^2}{(1 + g^2 - 2g\cos\theta)^{3/2}} = \sum_{l=0}^{N} (2l + 1) g^l P_l(\cos\theta), \tag{11}$$

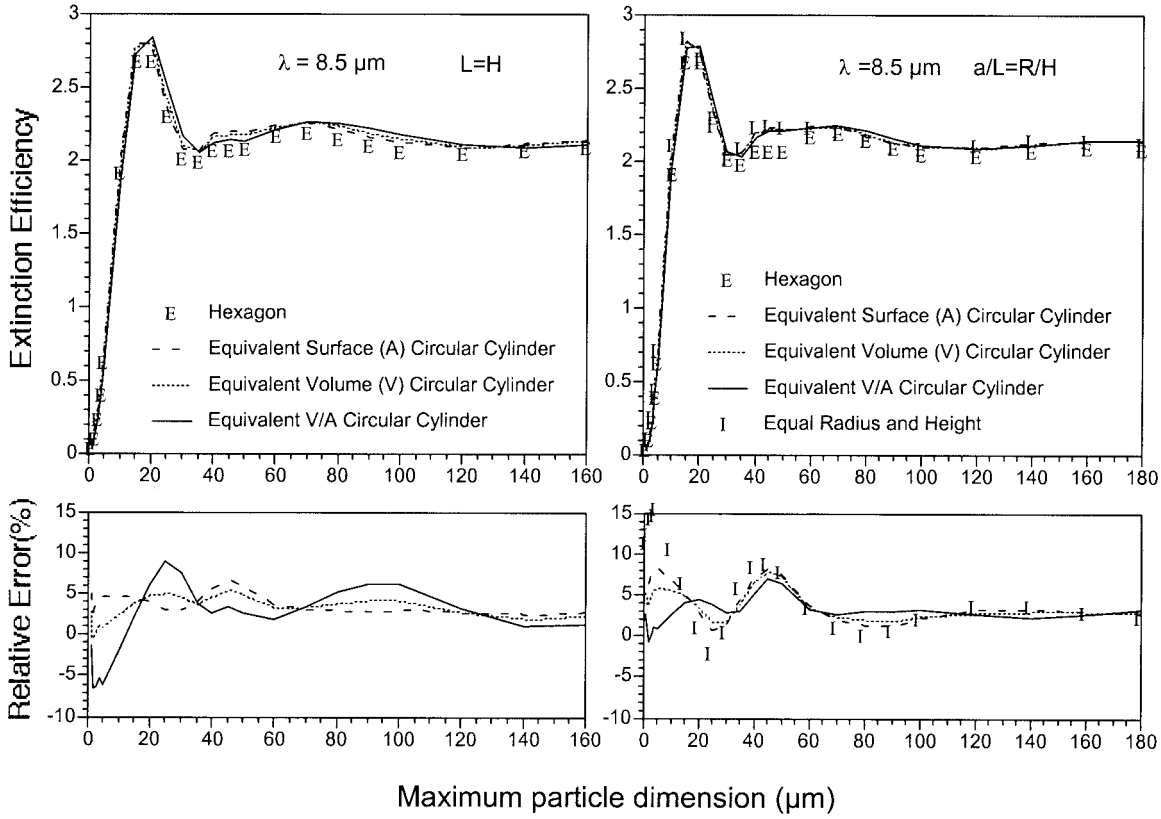

Fig. 3. Comparison of extinction efficiencies at a wavelength of 8.5 μm for hexagonal columns and various equivalent circular cylinders. The results for hexagonal particles are taken from Yang *et al.*[50]

where θ is the scattering angle and g is the asymmetry factor of ice crystal, which is defined as

$$g = \tfrac{1}{2}\int_0^{\pi} P(\theta)\cos(\theta)\sin(\theta)\mathrm{d}\theta, \qquad (12)$$

where $P(\theta)$ is the phase function of nonspherical ice crystals. $P_l(\cos\theta)$ in Eq. (11) is the lth Legendre polynomial. The Henyey–Greenstein phase function is used frequently for its simplicity and efficiency in numerical computations. In the following discussion, emphasis will be given to the asymmetry factor of the phase function instead of to the detailed angular variation of the computed scattering phase function. Note that the present computations are limited to scalar optical properties. The computation of the full phase matrix elements of the circular ice cylinders at a number of infrared wavelengths was recently reported by Xu *et al.*,[54] who used Mishchenko's T-matrix code for their numerical computation.

The present computations cover the terrestrial infrared window (8–12-μm) region, but in this paper the discussion is limited to numerical results at 8.5- and 11-μm wavelengths. The radiometric measurements at the spectral bands centered at these two wavelengths are often used to retrieve cloud properties.[14] For investigations involving ice particles, the 11-μm wavelength is unique because it is within the Christiansen band.[55,56] To ascertain the differences between the optical properties of circular ice cylinders and hexagonal ice columns, we define the relative difference ε as follows:

$$\varepsilon = \frac{\mathrm{Result}_{\mathrm{circ\ cyl}} - \mathrm{Result}_{\mathrm{hexag\ col}}}{\mathrm{Result}_{\mathrm{hexag\ col}}} \times 100\%. \qquad (13)$$

Figure 3 shows the extinction efficiencies of hexagonal ice columns and various equivalent circular ice cylinders at λ = 8.5 μm. Also shown are the relative differences between the results for the hexagonal and the circular cylinder geometries. At the left, the hexagons and the circular cylinders have the same length; at the right, the two geometries have the same aspect ratio. Evidently, for large particles (>120 μm) the differences among various equivalent definitions are reduced in magnitude, particularly when the aspect ratio is kept constant for the two geometries. The extinction efficiency of the equivalent-volume circular cylinder ($L = H$) is closer than other equivalence definitions to that of a hexagonal column. The maximum difference is less than 10%, except when the two geometries have the same length and radius. For large sizes (>100 μm) the maximum difference is reduced to approximately 3%. In a previous study Baran and Havemann[57] noticed that for large size parameters the single-scattering properties become asymptotic to their limiting values

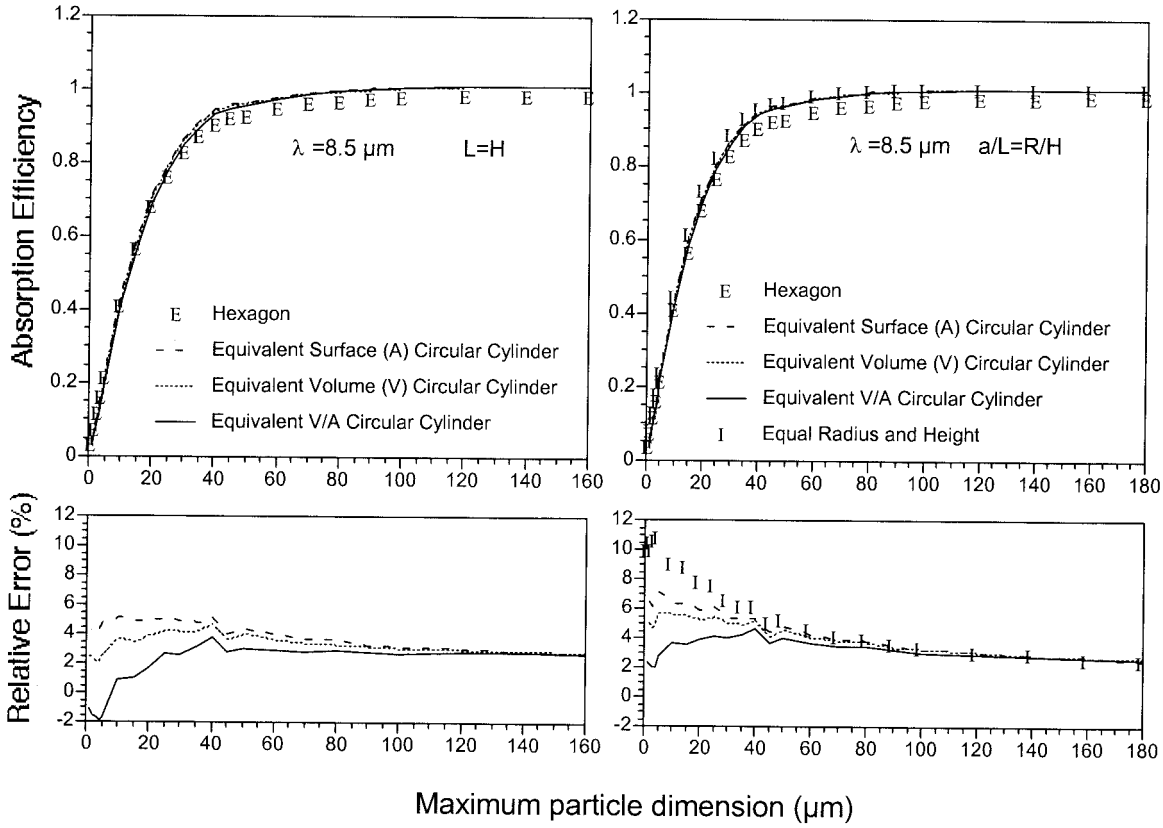

Fig. 4. Absorption efficiencies that correspond to the extinction efficiencies shown in Fig. 3.

and as such become independent of crystal shape at infrared wavelengths.

Figure 4 shows the absorption efficiencies and relative differences that correspond to the results shown in Fig. 3. Evidently, for large particle sizes (>100 μm) the results for various definitions of equivalent circular cylinders converge, and the relative differences converge to approximately 2%. The differences between the absorption efficiency of hexagonal columns and that of the circular cylinders with the same ratio of volume to projected area are smaller than the results for other equivalence definitions. Fu *et al.*[36] ascertained the errors of approximating hexagonal columns by spheres with various equivalent definitions in the computation of absorption efficiency. They also noticed that the equivalent sphere based on the same ratio of volume to projected area leads to the smallest errors. Our conclusion is consistent with the previous study. For practical applications of infrared radiative transfer, the most important process is absorption. From this perspective, hexagonal ice columns may be approximated by circular cylinders with the same ratio of volume to projected area. In fact, the ratio of particle volume to particle projected area is proportional to the mean path length of the rays inside particle in the framework of anomalous diffraction theory.

Figure 5 shows the asymmetry factor values that correspond to the extinction and absorption efficiencies shown in Figs. 3 and 4. The definition of the equivalent circular cylinder for a hexagonal column seems to have a negligible effect on the value of the asymmetry factor when the particle size is larger than approximately 80 μm. In this case the differences of the asymmetry factors between the hexagonal and circular cylinder geometries are less than 2%. For particle sizes smaller than 20 μm it is important how the equivalent circular cylinder is defined. When $L = H$, the asymmetry factor for the equivalent-volume circular cylinders is closer than the other equivalent circular cylinder definitions to that of hexagonal columns. Another property shown in Fig. 5 is that the asymmetry factor is small for small particles (less than 15 μm), whereas the asymmetry factor reaches its asymptotic value for large particle sizes. For small particles, the scattering pattern is close to that of Rayleigh scattering and the phase function is not strongly asymmetric with respect to scattering angle, leading to a small asymmetry factor. When the particle size is large, any rays refracted into the particles are essentially absorbed because of the strong absorption of ice at infrared wavelengths. The scattered energy is derived primarily from the diffracted energy that is concentrated in the forward direction.

Figures 6, 7, and 8 show the extinction efficiency, the absorption efficiency, and the asymmetry factor, respectively, but at $\lambda = 11$ μm. The Christiansen band lies near 11 μm.[55,56] In this region the extinction reaches its minimum and the absorption within

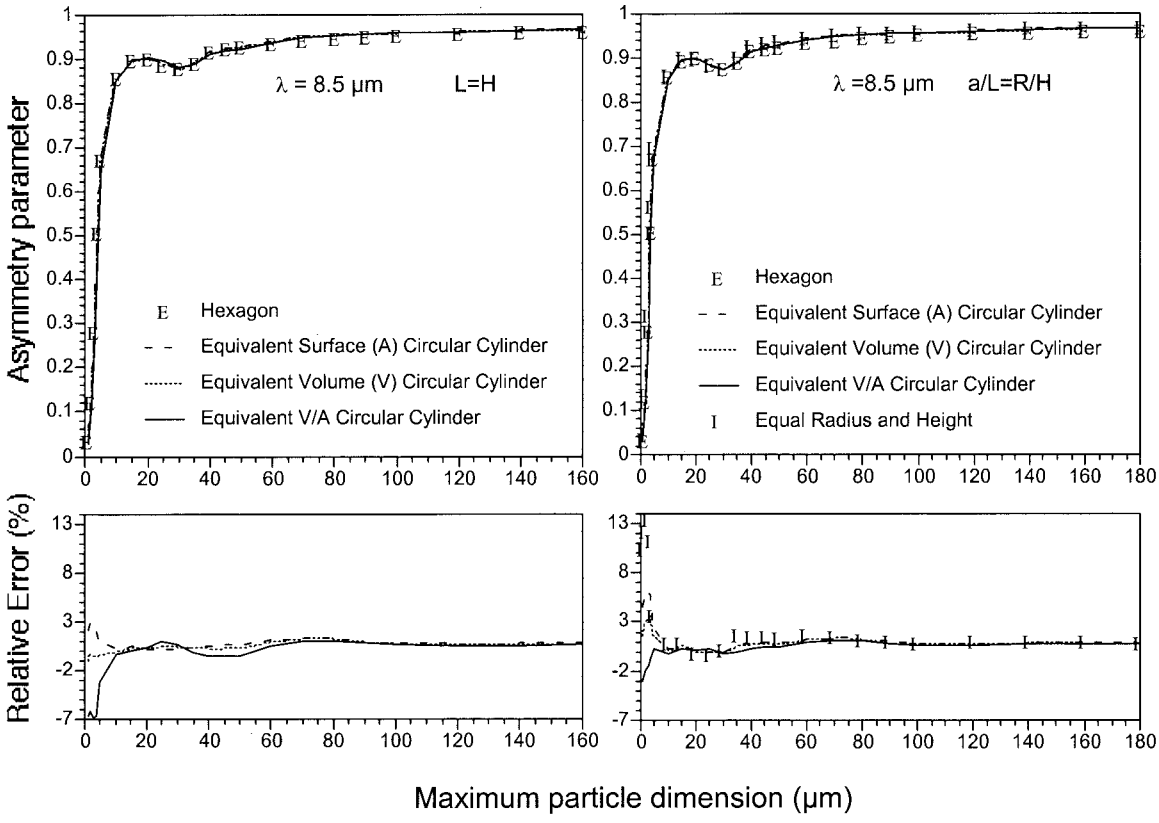

Fig. 5. Asymmetry factors that correspond to the efficiencies shown in Figs. 3 and 4.

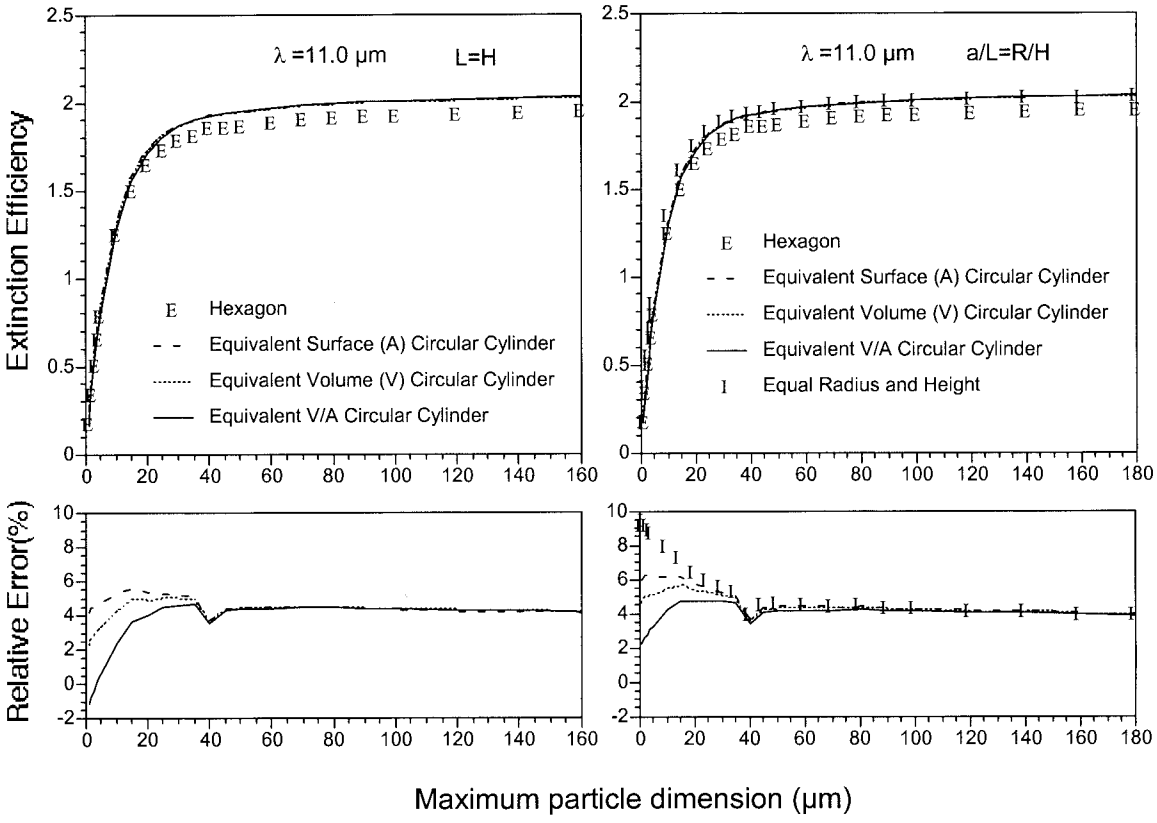

Fig. 6. Same as Fig. 3, except that the calculations are performed at a wavelength of 11 μm.

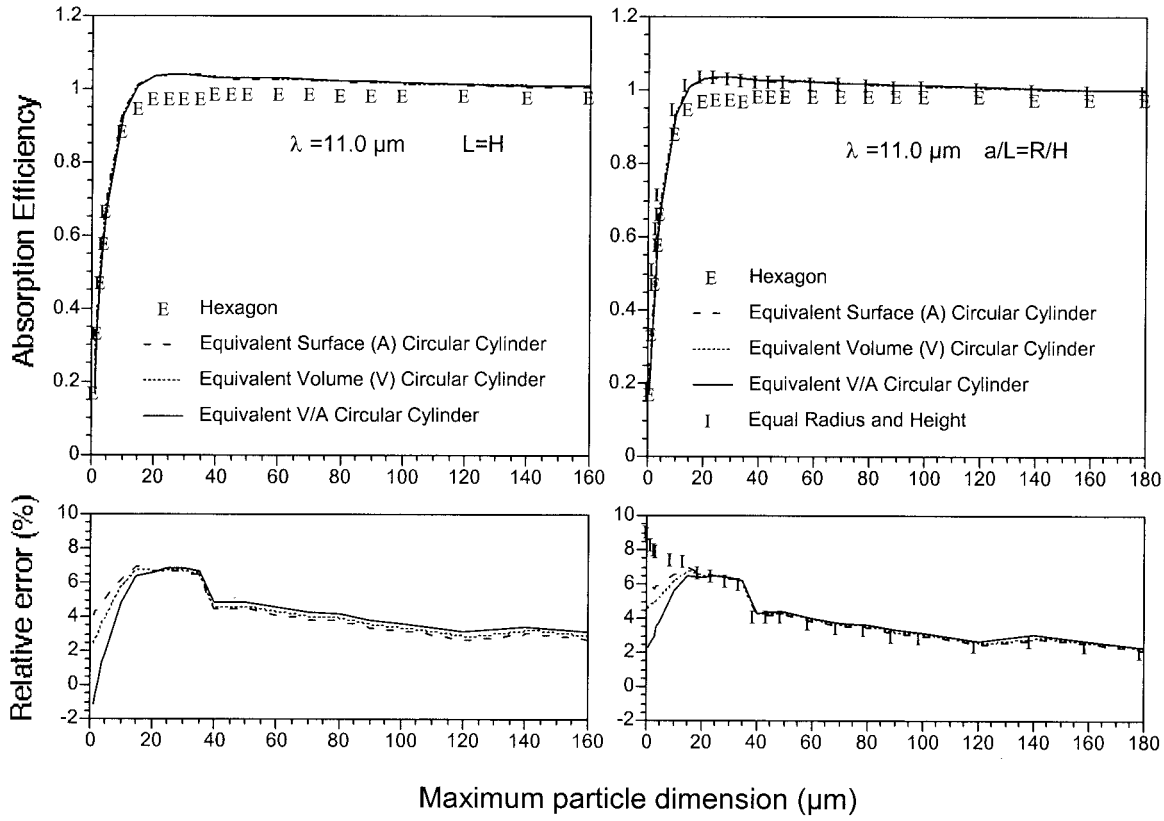

Fig. 7. Same as Fig. 4, except that the calculations are performed at a wavelength of 11 μm.

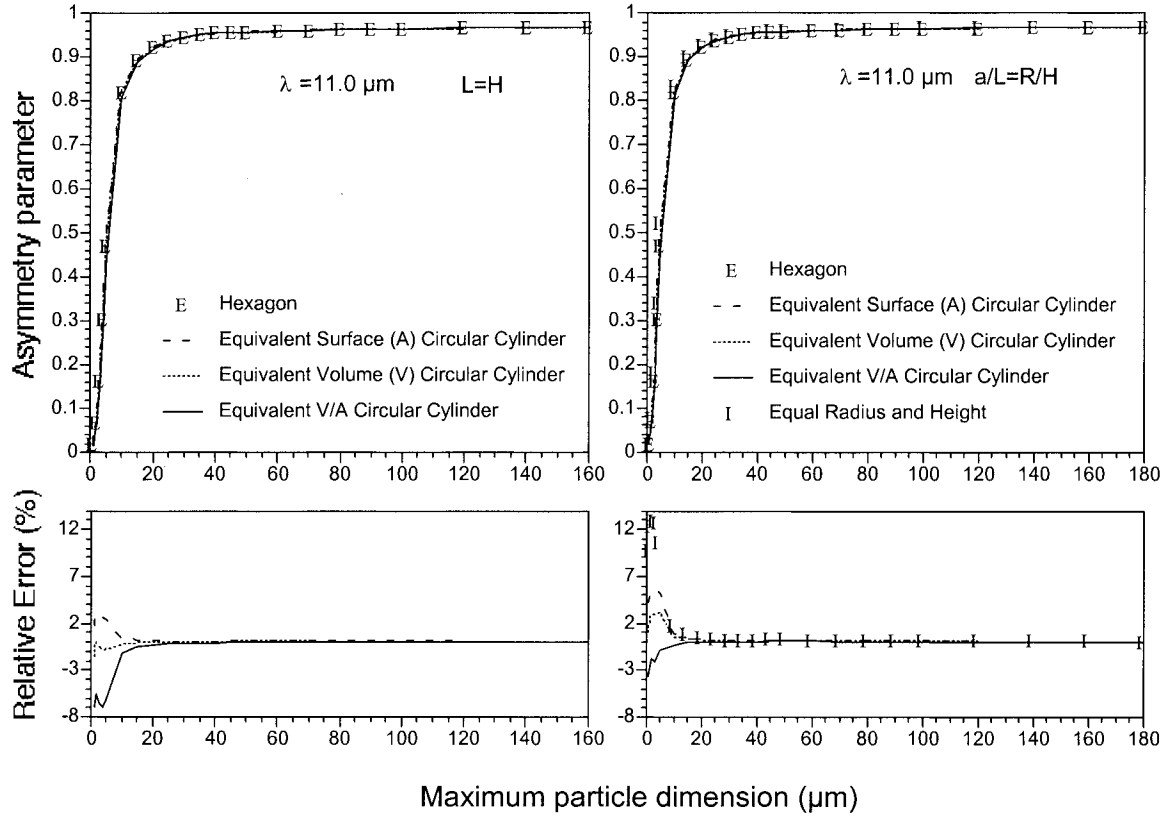

Fig. 8. Same as Fig. 5, except that the calculations are performed at a wavelength of 11 μm.

Table 1. Minimum and Maximum Relative Errors of the Approximation of Hexagonal Column by a Circular Cylinder by Use of a T Matrix Compared with Reference Results Given by Yang *et al.*[a]

Property	$H = L$			$a/L = R/H$			
	Equivalent Surface Area (A)	Equivalent Volume (V)	Equivalent Ratio of V to A	Equivalent Surface Area (A)	Equivalent Volume (V)	Equivalent Ratio of V to A	$a = R$ and $H = L$
$\lambda = 8.5$ μm							
Extinction efficiency	(2.4, 6.6)	(−0.6, 5.5)	(−6.5, 8.9)	(0.7, 8.4)	(1.7, 7.8)	(−0.7, 7.0)	(−2.0, 15.5)
Absorption efficiency	(2.7, 5.2)	(2.1, 4.7)	(−1.9, 3.8)	(2.5, 7.1)	(2.5, 5.7)	(2.0, 4.6)	(2.5, 10.8)
Asymmetry factor	(0.1, 2.9)	(−0.1, 1.2)	(−6.9, 1.0)	(−0.1, 6.2)	(−0.2, 3.6)	(−3.0, 1.2)	(−0.4, 13.4)
$\lambda = 11$ μm							
Extinction efficiency	(3.8, 5.6)	(2.3, 5.0)	(−1.2, 4.7)	(3.9, 6.2)	(3.9, 5.7)	(2.2, 4.8)	(3.9, 9.5)
Absorption efficiency	(2.7, 6.9)	(2.3, 6.8)	(−1.1, 6.9)	(2.1, 7.0)	(2.2, 6.8)	(2.3, 6.5)	(2.0, 9.1)
Asymmetry factor	(0.0, 3.1)	(−1.8, 0.2)	(−6.9, 0.1)	(−0.1, 5.7)	(0.1, 3.2)	(−3.6, 0.2)	(0.1, 12.8)

[a]Ref. 50.

the ice crystal is substantial. Unlike at $\lambda = 8.5$ μm, the extinction efficiency at $\lambda = 11$ μm converges for various definitions of equivalent circular cylinders for particle sizes larger than 60 μm. The asymptotic value for the differences between the extinction efficiencies of the hexagonal column and the circular cylinder is approximately 4%.

For the absorption efficiency shown in Fig. 7, the results for the equivalent volume, the equivalent surface area, and the equivalent ratio of volume to surface area yield similar differences. All three definitions yield a maximum relative difference in the size range 15–40 μm. However, the magnitude of the differences is less than 7%. For very small ice crystals, with sizes from 1 to 10 μm, the equivalence based on equal radius and height can lead to differences much larger than differences for other definitions. For the asymmetry factor shown in Fig. 8, convergence of the results for various equivalence definitions is obtained for particle sizes larger than 20 μm. For small sizes (<20 μm), the equivalent-volume circular cylinder yields the minimum difference when the two geometries have the same length (i.e., $L = H$).

Table 1 lists the errors obtained from approximating hexagonal columns by circular cylinders based on the calculation of the various optical properties shown in Figs. 3–8. Based on these error values, the equivalence based on the ratio V/A performs the best for calculation of the absorption efficiency. For the asymmetry factor the volume equivalence definition yields the minimum errors. For extinction efficiency, various equivalence definitions have a similar error range, except when the equivalence is based on $a = R$ and $H = L$.

In reality, pristine ice crystals are not common in cirrus clouds. For ice crystals with complex geometries, their optical properties cannot be well approximated by those of a simple morphological structure. To illustrate this, in Fig. 9 we show the absorption efficiencies of pristine hexagonal columns and aggregates. The definition of the aggregate geometry is explained by Yang and Liou.[58] The numerical computation of the optical properties of aggregates in Fig. 9 is explained by Yang *et al.*[59] Following Foot,[12] Francis *et al.*,[60] Mitchell and Arnott,[61] and Fu *et al.*,[36] we define the effective radius as

$$R_e = \frac{3}{4}\frac{V}{A}, \tag{14}$$

where V and A are the volume and the projected area, respectively, of the nonspherical particles. From Fig. 9 it is evident that the absorption efficiencies of the two geometries are quite different, regardless of whether the sizes of the particles are defined in terms of maximum dimension or effective size. Note that Baran *et al.*[62] ascribe the differences in the absorption efficiencies of aggregates and columns to a tunneling effect.

4. Conclusions

The accuracy of approximating hexagonal crystals by circular cylinders has been investigated in the computation of the scalar optical properties of pristine ice crystals in the infrared spectral (8–12-μm) region. Various definitions were used to define the equivalence of particles in a circular cylinder with those of a hexagonal column. The T-matrix computational program was used to solve for the single-scattering properties of circular cylinders.

For extinction efficiency, absorption efficiency, and asymmetry, the differences between the results for the two geometries are less than 10%. In general, errors for particles of sizes smaller than 20 μm are more significant than the errors for larger particles. For particle sizes larger than 40 μm, the differences are essentially of the order of a few percent. At $\lambda = 8.5$ μm, the circular cylinder with an equivalent volume-to-surface ratio to that of a hexagonal column yields a smaller difference in the computation of absorption efficiency than do equivalent-volume or equivalent-surface circular cylinders. This difference is particularly pronounced for particle sizes less than 40 μm. At $\lambda = 11$ μm, the definition of equivalence for a circular cylinder has a negligible effect on

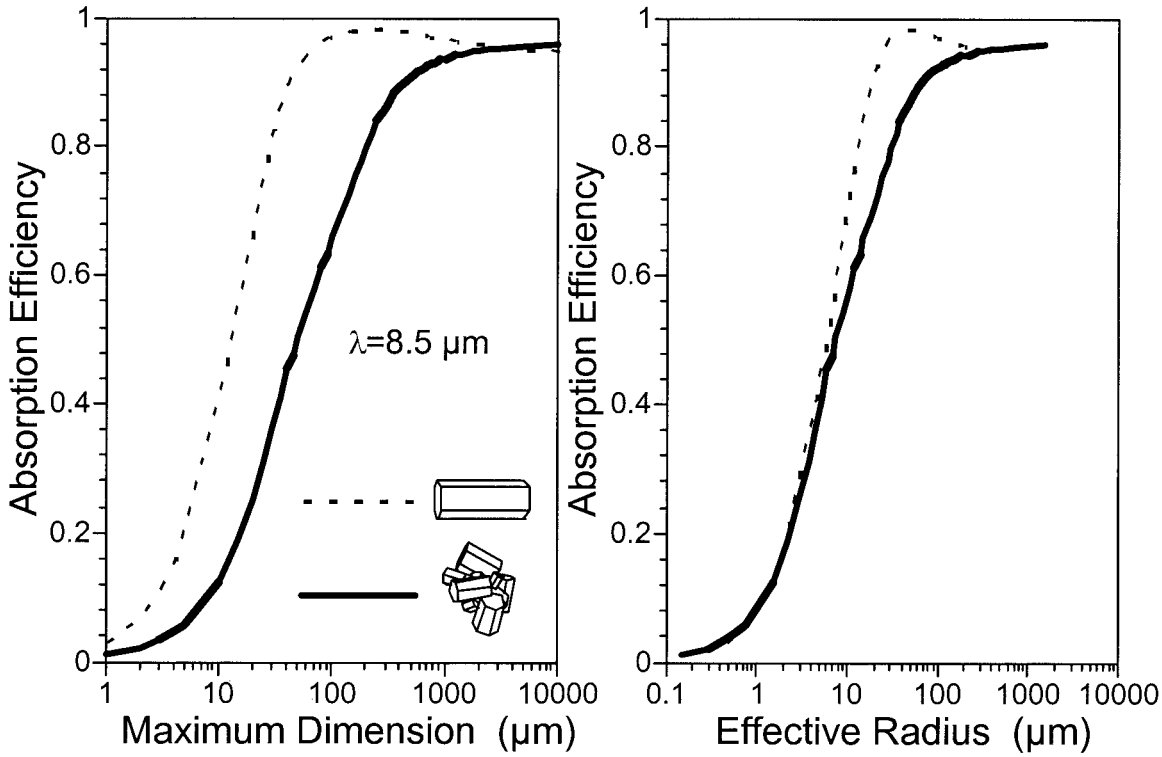

Fig. 9. Comparison of absorption efficiencies of pristine hexagonal ice columns and aggregate ice crystals. The procedure for computing the optical properties of aggregates was explained by Yang *et al.*[59]

the calculation of absorption efficiency when particle sizes are larger than 15 μm. A detailed comparison of the numerical computations associated with various equivalence definitions of circular cylinders indicates that the equivalence based on the ratio V/A is most suitable for absorption efficiency when the two geometries have the same aspect ratio ($a/L = R/H$) and the volume equivalence is suitable for asymmetry factor or phase function calculations when the two geometries have the same length ($L = H$). The error ranges for equivalence-area, equivalent-volume, and equivalent V/A are slightly different in the computation of extinction efficiency. In general, the errors associated with the use of circular cylinders as surrogates for hexagonal ice crystals in scattering calculations at infrared wavelengths are of the order of a few percent. Thus it quite reasonable to approximate the geometry of pristine ice crystals as circular cylinders in the study of infrared radiation.

It has also been shown that it is not proper to approximate a complex aggregate geometry with a simplified geometry such as a hexagonal column for computing optical properties. Because aggregates and bullet rosettes are common in cirrus clouds, there is a need to include their particle geometry in modeling of the optical properties of cirrus particles, even at infrared wavelengths. Future research will explore a surrogate particle that better approximates the more-complex crystal geometries found in nature. In particular, it will be worthwhile to investigate whether it is valid to approximate an aggregate ice crystal by using a number of individual cylinders based on the method developed by Grenfell and Warren,[35] who suggested an equivalence of a circular cylinder and a monodisperse sphere (with the same volume-to-surface ratio) system for scattering and radiative transfer computations.

This study was supported by research grants NAG-1-02002 and NAG5-11374 from the NASA Radiation Sciences Program managed by Donald Anderson and also by U.S. Office of Naval Research Multidisciplinary Research Program of the University Research Initiative funded through the Navy Indian Ocean METOC Imaging mission for the Geostationary Imaging Fourier Transform Spectrometer project as well as the NASA Cloud-Aerosol Lidar and Infrared Pathfinder Satellite Observations project. A. J. Baran is partially funded by the U.K. Department of Environment, Food and Rural Affairs under contract PECD 7/12/37.

References and Notes

1. K. N. Liou, "Influence of cirrus clouds on weather and climate processes: a global perspective," Mon. Weather Rev. **114,** 1167–1199 (1986).
2. G. L. Stephens, S. C. Tsay, P. W. Stackhouse, and P. J. Flatau, "The relevance of the microphysical and radiative properties of cirrus clouds to climate and climate feedback," J. Atmos. Sci. **47,** 1742–1753 (1990).
3. J. E. Kristjansson, J. M. Edwards, and D. L. Mitchell, "The impact of a new scheme for optical properties of ice crystals on the climate of two GCMs," J. Geophys. Res. **105,** 10,063–10,079 (2000).

4. A. J. Heymsfield and J. Iaquinta, "Cirrus crystal terminal velocities," J. Atmos. Sci. **57,** 916–938 (2000).
5. A. J. Heymsfield, S. Lewis, A. Bansemer, J. Iaquinta, L. M. Miloshevich, M. Kajikawa, C. Twohy, and M. R. Poellot, "A general approach for deriving the properties of cirrus and stratiform ice cloud particles," J. Atmos. Sci. **59,** 3–29 (2002).
6. W. P. Arnott, Y. Y. Dong, J. Hallett, and M. R. Poellot, "Role of small ice crystals in radiative properties of cirrus: a case study, FIRE II, November 22, 1991," J. Geophys. Res. **99,** 1371–1381 (1994).
7. D. L. Mitchell, A. Macke, and Y. Liu, "Modeling cirrus clouds. II. Treatment of radiative properties," J. Atmos. Sci. **53,** 2967–2988 (1996).
8. Y. Takano and K. N. Liou, "Radiative transfer in cirrus clouds. II. Theory and computation of multiple scattering in an anisotropic medium," J. Atmos. Sci. **46,** 20–36 (1989).
9. Y. Takano and K. N. Liou, "Solar radiative transfer in cirrus clouds. I. Single-scattering and optical properties of hexagonal ice crystals," J. Atmos. Sci. **46,** 3–19 (1989).
10. E. E. Ebert and J. A. Curry, "A parameterization of ice cloud optical properties for climate models," J. Geophys. Res. **97,** 3831–3836 (1992).
11. Q. Fu, "An accurate parameterization of the solar radiative properties of cirrus clouds for climate models," J. Clim. **9,** 2058–2082 (1996).
12. J. S. Foot, "Some observations of the optical properties of clouds. II. Cirrus," Q. J. R. Meteorol. Soc. **114,** 145–164 (1988).
13. K. Wyser and P. Yang, "Average crystal size and bulk shortwave single scattering properties in ice clouds," Atmos. Res. **49,** 315–335 (1998).
14. B. A. Baum, D. Kratz, P. Yang, S. C. Ou, Y. X. Hu, P. F. Soulen, and S. C. Tsay, "Remote sensing of cloud properties using MODIS airborne simulator imagery during SUCCESS. 1. Data and models," J. Geophys. Res. **105,** 11767–11780 (2000).
15. P. Yang, B.-C. Gao, B. A. Baum, W. Wiscombe, Y. Hu, S. Nasiri, P. Soulen, A. Heymsfield, G. McFarquhar, and L. Miloshevich, "Sensitivity of cirrus bidirectional reflectance to vertical inhomogeneity of ice crystal habits and size distributions for two Moderate-Resolution Imaging Spectroradiometer (MODIS) bands," J. Geophys. Res. **106,** 17267–17291 (2001).
16. G. M. McFarquhar, P. Yang, A. Macke, and A. J. Baran, "A new parameterization of single-scattering solar radiative properties for tropical anvils using observed ice crystal size and shape distributions," J. Atmos. Sci. **59,** 2458–2478 (2002).
17. M.-D. Chou, K.-T. Lee, and P. Yang, "Parameterization of shortwave cloud optical properties for a mixture of ice particle habits for use in atmospheric models," J. Geophys. Res. **107,** doi: 10.109/2002JD002061 (2002).
18. J. R. Key, P. Yang, B. A. Baum, and S. L. Nasiri, "Parameterization of shortwave ice cloud optical properties for various particle habits," J. Geophys. Res. **107,** 10.1029/2001JD000742 (2002).
19. C. F. Bohren and D. R. Huffman, *Absorption and Scattering of Light by Small Particles* (Wiley, New York, 1983).
20. P. Yang and K. N. Liou, "Light scattering by hexagonal ice crystals: comparison of finite-difference time domain and geometric optics methods," J. Opt. Soc. Am. A **12,** 162–176 (1995).
21. P. Yang, B.-C. Gao, B. A. Baum, Y. X. Hu, W. Wiscombe, M. I. Mischenko, D. M. Winker, and S. L. Nasiri, "Asymptotic solutions of optical properties of large particles with strong absorption," Appl. Opt. **40,** 1532–1547 (2001).
22. A. Taflove, *Computational Electrodynamics: The Finite-Difference Time-Domain Method* (Artech House, Boston, Mass., 1995).
23. P. Yang and K. N. Liou, "Finite-difference time domain method for light scattering by small ice crystals in three-dimensional space," J. Opt. Soc. Am. A **13,** 2072–2085 (1996).
24. W.-B. Sun, Q. Fu, and Z. Chen, "Finite-difference time-domain solution of light scattering by dielectric particles with a perfectly matched layer absorbing boundary condition," Appl. Opt. **38,** 3141–3151 (1999).
25. P. Yang, K. N. Liou, M. I. Mishchenko, and B.-C. Gao, "An efficient finite-difference time domain scheme for light scattering by dielectric particles: application to aerosols," Appl. Opt. **39,** 3727–3737 (2000).
26. E. M. Purcell and C. R. Pennypacker, "Scattering and absorption of light by nonspherical dielectric grains," Astrophys. J. **186,** 705–714 (1973).
27. B. T. Draine, "The discrete-dipole approximation and its application to interstellar graphite grains," Astrophys. J. **333,** 848–872 (1988).
28. B. T. Draine and P. J. Flatau, "Discrete-dipole approximation for light calculations," J. Opt. Soc. Am. A **11,** 1491–1499 (1994).
29. M. I. Mishchenko, J. W. Hovenier, and L. D. Travis, *Light Scattering by Nonspherical Particles: Theory, Measurements, and Applications* (Academic, San Diego, Calif., 2000).
30. K. N. Liou and Y. Takano, "Light scattering by nonspherical particles: remote sensing and climatic implications," Atmos. Res. **31,** 271–298 (1994).
31. P. Chylek and G. Videen, "Longwave radiative properties of polydispersed hexagonal ice crystal," J. Atmos. Sci. **51,** 175–190 (1994).
32. A. Macke and M. I. Mishchenko, "Applicability of regular particle shapes in light scattering calculations for atmospheric ice particles," Appl. Opt. **35,** 4291–4296 (1996).
33. F. M. Kahnert, J. J. Stamnes, and K. Stamnes, "Can simple particle shapes be used to model scalar optical properties of an ensemble of wavelength-sized particles with complex shapes?" J. Quant. Spectrosc. Radiat. Transfer **19,** 521–531 (2002).
34. A. J. Baran, P. N. Francis, P. Yang, and S. Havemann, "Simulation of scattering from ice aggregates using size/shape distributions of circular ice cylinders: an application of T-matrix," in *Proceedings of the Sixth Conference on Light Scattering by Nonspherical Particles*, B. Gustafson, L. Kolokolova, and G. Videen, eds. (Army Research Laboratory, Adelphi, Md., 2002), pp. 25–28.
35. T. C. Grenfell and S. G. Warren, "Representation of a nonspherical ice particle by a collection of independent spheres for scattering and absorption of radiation," J. Geophys. Res. **104,** 31697–31709 (1999).
36. Q. Fu, P. Yang, and W. B. Sun, "An accurate parameterization of the infrared radiative properties of cirrus clouds for climate models," J. Clim. **11,** 2223–2237 (1998).
37. Q. Fu, W. B. Sun, and P. Yang, "Modeling of scattering and absorption by cirrus nonspherical ice particles at thermal infrared wavelengths," J. Atmos. Sci. **56,** 2937–2947 (1999).
38. M. I. Mishchenko, "Light scattering by randomly oriented axially symmetric particles," J. Opt. Soc. Am. A **8,** 871–882 (1991).
39. M. I. Mishchenko and L. D. Travis, "Capabilities and limitations of a current FORTRAN implementation of the T-matrix method for randomly oriented, rotationally symmetric scatterers," J. Quant. Spectrosc. Radiat. Transfer **60,** 309–324 (1998).
40. P. C. Waterman, "Matrix formulation of electromagnetic scattering," Proc. IEEE **53,** 805–812 (1965).
41. W. J. Wiscombe and A. Mugnai, "Scattering from nonspherical Chebyshev particles. 2. Means of angular scattering patterns," Appl. Opt. **27,** 2405–2421 (1986).
42. P. W. Barber and S. C. Hill, *Light Scattering by Particles: Computational Methods* (World Scientific, Singapore, 1990).
43. T. Wriedt and A. Doicu, "Formulations of the extended boundary condition method for three-dimensional scattering using

the method of discrete sources," J. Mod. Opt. **45,** 199–213 (1998).
44. H. Laitinen and K. Lumme, "T-matrix method for general star-shaped particles: first results," J. Quant. Spectrosc. Radiat. Transfer **60,** 325–334 (1998).
45. D. W. Mackowski and M. I. Mishchenko, "Calculation of the T-matrix and the scattering matrix for ensembles of spheres," J. Opt. Soc. Am. A **13,** 2266–2278 (1996).
46. S. Havemann and A. J. Baran, "Extension of T-matrix to scattering of electromagnetic plane waves by non-axisymmetric dielectric particles: application to hexagonal ice cylinders," J. Quant. Spectrosc. Radiat. Transfer **70,** 139–158 (2001).
47. D. W. Mackowski, "Discrete dipole moment method for calculation of the T matrix for nonspherical particles," J. Opt. Soc. Am. A **19,** 881–893 (2002).
48. G. Videen, Army Research Laboratory AMSRL-CI-EE, 2800 Powder Mill Road, Adelphi, Md. 20783-1197 (personal communication, 2002).
49. M. I. Mishchenko, "Light scattering by size-shape distributions of randomly oriented axially symmetric particles of a size comparable to a wavelength," Appl. Opt. **32,** 623–625 (1993).
50. P. Yang, B. C. Gao, B. A. Baum, Y. X. Hu, W. J. Wiscombe, S. C. Tsay, D. M. Winker, and S. L. Nasiri, "Radiative properties of cirrus clouds in the infrared (8–13 μm) spectral region," J. Quant. Spectrosc. Radiat. Transfer **70,** 473–504 (2001).
51. S. G. Warren, "Optical constants of ice from the ultraviolet to the microwave," Appl. Opt. **23,** 1206–1225 (1984).
52. M. I. Mishchenko and L. D. Travis, "T-matrix computations of light scattering by large spheroidal particles," Opt. Commun. **109,** 16–21 (1994).
53. A. J. Baran, P. Yang, and S. Havemann, "Calculation of the single-scattering properties of randomly oriented hexagonal ice columns: a comparison of the T-matrix and the finite-difference time-domain methods," App. Opt. **40,** 4376–4386 (2001).
54. L. Xu, J. Ding, and A. Cheng, "Scattering matrix of infrared radiation by ice finite circular cylinders," Appl. Opt. **41,** 2333–2348 (2002).
55. W. P. Arnott, Y. Y. Dong, and J. Hallett, "Extinction efficiency in the infrared (2–18 μm) of laboratory ice clouds: observations of scattering minima in the Christiansen bands of ice," Appl. Opt. **34,** 541–551 (1995).
56. P. Yang, K. N. Liou, and W. P. Arnott, "Extinction efficiency and single-scattering albedo of ice crystals in laboratory and natural cirrus clouds," J. Geophys. Res. **102,** 21825–21835 (1997).
57. A. J. Baran and S. Havemann, "Comparison of electromagnetic theory and various approximations for computing the absorption efficiency and single-scattering albedo of hexagonal columns," Appl. Opt. **39,** 5560–5568 (2000).
58. P. Yang and K. N. Liou, "Single-scattering properties of complex ice crystals in terrestrial atmosphere," Contrib. Atmos. Phys. **71,** 223–248 (1998).
59. P. Yang, B. A. Baum, H.-L. Huang, S. Platnick, Y. X. Hu, D. M. Winker, A. J. Baran, and P. N. Francis, "Single and multiple scattering/absorption properties of pristine ice crystals and polycrystals in the terrestrial window region," in *Proceedings of the Sixth Conference on Light Scattering by Nonspherical Particles*, B. Gustafson, L. Kolokolova, and G. Videen, eds. (Army Research Laboratory, Adelphi, Md., 2002), pp. 369–372.
60. P. N. Francis, A. Jones, R. W. Saunders, K. P. Shine, A. Slingo, and Z. Sun, "An observational and theoretical study of the radiative properties of cirrus: some results from ICE'89," Q. J. R. Meteorol. Soc. **120,** 809–848 (1994).
61. D. L. Mitchell and W. P. Arnott, "A model prediction the evolution of ice particle size spectra and radiative properties of cirrus cloud. II. Dependence of absorption and extinction on ice crystal morphology," J. Atmos. Sci. **51,** 817–832 (1994).
62. A. J. Baran, P. Francis, and P. Yang, "A process study of the dependence of ice crystal absorption on particle geometry: application to aircraft radiometric measurements of cirrus clouds in the terrestrial window region," J. Atmos. Sci. (to be published).